Reconciling surrogate-reaction probabilities and neutron-induced cross sections

O. Bouland* and G. Noguère
CEA, DES, IRESNE, DER, SPRC, Physics Studies Laboratory, Cadarache, F-13108 Saint-Paul-lez-Durance, France

(Received 27 March 2020; accepted 9 October 2020; published 17 November 2020)

Since its inception, the so-called *surrogate-reaction method* (SRM) has motivated the development and improvement of theories in connection to direct reactions. This paper reassesses some of the developments carried out in previous decades to deal with the representation of direct reaction probability data. It is believed that the experimental probabilities assimilation in the neutron cross section evaluation process can be better estimated using tools resulting from the efforts made over the years. This paper provides a new perspective on this issue both in terms of fission and γ-ray emission probabilities. In addition to the "natural" assimilation path that considers analyzing probabilities jointly with cross sections to extract nuclei structural properties, this article puts forward a prescription to convert, with a good level of confidence, measured direct-reaction induced probabilities to pseudoexperimental neutron-induced cross sections. This approach is named after the SRM as *extended SRM* (ESRM).

DOI: 10.1103/PhysRevC.102.054608

I. INTRODUCTION

Neutron-induced cross section evaluation methods have achieved a large degree of proficiency whereby it becomes more and more difficult to improve the outcome result. Therefore, the reduction of nuclear data uncertainties will require further steps, such as the inclusion of observables other than cross sections in the experimental evaluation database. Among those are deexcitation probabilities induced by *direct reactions*. A direct reaction is commonly associated with a short-time interaction between a projectile and a target nucleus. It occurs across a two-body collision involving the projectile and one nucleon of the target. Raised to an unfilled level, the nucleon subsequently escapes from the excited nucleus. Alternatively, an intermediate-stage *compound nucleus* may be formed whenever the struck nucleon does not leave, but rather triggers a series of two-body collisions. According to this picture, the entire kinetic energy of the projectile is spread among the nucleons of the projectile-target combination. Direct reactions are thus more selective than compound nucleus excitations since they directly connect the nuclear states of both the target and residual nuclei. The stripping (d, p) reaction is a well-known example of direct reactions that has been exhaustively studied starting from the 1930s [1].

The idea to supplement neutron-induced cross-section data with particle-transfer induced reactions was raised a long time ago and began with fission probability measurements on the actinides and higher transuranic nuclides [2]. The benefit of this technique shows up clearly for neutron target material with unsuitable lifetimes (less than several days) or with high radiotoxicity. Since for heavy nuclides the fission barrier lies below the neutron separation energy (S_n), direct reactions supply also invaluable feedback on the fluctuating shape [3] of the fission potential barrier (height and curvature) and the nature of transition states [4] (quantum numbers and energies) lying on top of the barrier.

Fission probability data have been analyzed assuming several simplifications contained in the so-called *surrogate-reaction method* (SRM). This method appeared to operate reasonably well for major actinides [2] and "exotic" nuclei [5]. Since the 2000s, the direct-reaction induced probabilities have received renewed interest in terms of simulation [6,7] and experimental investigation (the study [8] was the first of this new series). The success of SRM was soon confirmed by its capability to infer the ^{241}Am, ^{242}Cm, and ^{243}Cm neutron fission cross sections [9].

The idea to apply the same method to infer neutron-induced radiative-capture cross sections ($\sigma_{n,\gamma}$) of target nuclei unsuitable for neutron spectroscopy followed, with efforts thus being made on the measurement of direct-reaction-induced γ-ray emission probabilities.

Neutron-induced capture cross sections are of prime importance in physics models, and in particular in those for nuclear-energy generation [11] and simulations of the astrophysical rapid and slow processes (r and s processes) [12]. Table I lists the estimated uncertainties of $\sigma_{n,\gamma}$ for some nuclides of interest in the fast neutron energy region from 200 keV to 1.3 MeV. In this energy range, performing a precise measurement remains very difficult via neutron spectroscopy. The estimates carried out for ^{239}Pu, ^{238}U, and ^{89}Y are representative of the current best knowledge on neutron-capture cross sections over this energy region whereas it is clear that for nuclides such as the medium-mass ^{90}Zr and ^{95}Mo much remains to be done. This illustrates the importance of our ability to model accurately measured γ-ray emission

*olivier.bouland@cea.fr

TABLE I. Neutron radiative-capture cross section uncertainties (%) as provided by COMAC-CEA V2.0 [10], the library of covariance matrices from Cadarache, regarding some nuclides of interest for nuclear physics over the fast neutron energy region.

Incident neutron	Neutron target nucleus				
energy range (keV)	^{89}Y	^{90}Zr	^{95}Mo	^{238}U	^{239}Pu
200–500	3	21	12	4	3
500–1300	8	24	15	5	8

probabilities to better constrain neutron-induced radiative capture cross sections even when neutron spectroscopy data are accessible. In the extreme case where neutron spectroscopy is highly unlikely, as for the very short-lived ^{243}Pu ($\tau_{1/2} = 4.95$ h), the availability of probability data brings a major benefit in the evaluation of the cross section. Indeed the ^{243}Pu capture cross section uncertainty, integrated over a light-water-reactor neutron spectrum, was estimated to be about 275% using the EAF2007/UN data library [13].

Because it is commonly agreed that $\sigma_{n,\gamma}$ is very difficult to predict without any experimental information, the use of a theoretical approach becomes attractive. In terms of theoretical development, a recent breakthrough [14] has been made in the computation of the γ-ray strength function following the experimental confirmation of the low-lying $M1$ *scissors mode* contribution [15]. Until then, the calculation of the radiative strength function S_γ, the ratio of the average capture width to the nuclear level mean spacing, required a normalization factor, often far from unity, to be consistent with the observed $\sigma_{n,\gamma}$.

Despite numerous efforts, the use of the SRM in the last decade to observed γ-ray probabilities has failed [16,17]. However, very recent advances [18,19], beyond the original SRM, have demonstrated significant progress in that matter. *In this paper, we wish to go further on the issue by giving up all the restrictive assumptions carried by the SRM. This results in a new prescription, in which all factors have been carefully weighted, to infer neutron-induced cross sections. It is described as "extended SRM" as a reference to the historical SRM.* Demonstration of the ESRM is made using the example of the ^{174}Yb(^{3}He, $p\gamma$)^{176}Lu* transfer reaction, carefully measured and described in [16]. The work presented here is particularly useful because of the recent experimental capability [20] to measure simultaneously fission and γ-ray probabilities for the same nuclear system. This dual configuration allows one to validate both the experimental setup and the analysis method used to extract the two probabilities because of the unitarity of the γ-ray emission probability below neutron emission and fission energy thresholds. Indeed, the normalization of some early-measured fission probability data is questionable [21].

II. THEORETICAL BACKGROUND

Direct reactions are used as substitute reactions to form the nucleus of interest, A^*, that is commonly formed by neutron spectroscopy as $n + (A-1) \rightarrow A^*$.[1] Alternatively, another projectile-target combination, more accessible experimentally in the case of target material with short lifetime or with high radiotoxicity, can be selected such that projectile + (surrogate target) $\rightarrow A^*$ + ejectile. By measuring the number of coincidences between the observable characterizing the deexcitation channel ($c' \equiv f, \gamma$) pursued and the *ejectile*, the experimental probability $\mathcal{P}^{A^*}_{\mathrm{surr},c'}$ is extracted as a function of E_x. More precisely, the ejectile signs the nucleus to be analyzed, E_x is the excitation energy in the center of mass of the compound system, and $\mathcal{P}^{A^*}_{\mathrm{surr},c'}$ is normalized to the total number of surrogate events recorded. The variety of *surrogate nuclear reactions* and the principle of the SRM have been reviewed in a very wide and detailed manner in [22]. We describe below only the key points of the method suggested in the 1970s to easily model the measured reaction probabilities.

The SRM-inferred neutron-induced cross section for the deexcitation channel (c') is simply expressed as the product

$$\sigma^{\mathrm{SRM}}_{n,c'}(E_n) = \sigma^{CN}_n(E_n)\, \mathcal{P}^{A^*}_{\mathrm{surr},c'}(E_x), \tag{1}$$

where $\sigma^{CN}_n(E_n) = \sum_{J^\pi} \sigma^{CN}_n(E_n, J^\pi)$ is the total compound nucleus (CN) neutron-induced formation cross section, summed over all J^π spin-parity populated states, at the incident neutron energy E_n. Equation (1) includes therefore two quantities: $\sigma^{CN}_n(E_n)$, *predicted* using a suitable neutron target optical model potential [23,24], and $\mathcal{P}^{A^*}_{\mathrm{surr},c'}$, the value of which is *experimentally* assessed.

In our AVXSF-LNG computer program [25,26], the two complementary types of measured observables, namely the deexcitation probability and the neutron-induced cross section, are computed using the same unique set of nuclear structure parameters. Two distinct methods, based on statistical Hauser-Feshbach theory [27], are implemented for any of the two observables: an analytical calculation and an efficient Monte Carlo algorithm. Neither of those two routes relies on the approximations carried by the SRM equation [Eq. (1)]. The Monte Carlo algorithm provides the most accurate results but will not be commented on here since it is not necessary for the present paper's demonstration. The analytical route, aiming to theoretically assess the measured quantity $\mathcal{P}^{A^*}_{\mathrm{surr},c'}$ of Eq. (1), is based on the following *three-factor equation*:

$$\mathcal{P}^{A^*}_{\mathrm{surr},c'}(E_x) = \sum_{J^\pi} \mathcal{F}^{A^*}_{\mathrm{surr}}(E_x, J^\pi) \mathcal{B}^{J^\pi}_{c'}(E_x) W^{J^\pi}_{\mathrm{surr},c'}(E_x), \tag{2}$$

where $W_{\mathrm{surr},c'}$ is a surrogate-reaction-dedicated factor, called SWFCF [26], that accounts for channel width fluctuation correlations across flux conservation [28]. $\mathcal{F}^{A^*}_{\mathrm{surr}}(E_x, J^\pi)$ is the fraction of the *compound system* (A^*) formed by direct interaction in a specific (J, π) state of excitation energy E_x and defined as the ratio $[\sigma^{CN}_n(E_n, J^\pi)/\sigma^{CN}_n(E_n)]$. Finally, $\mathcal{B}^{J^\pi}_{c'}$ is the branching ratio for the deexcitation channel c'. Equation (2) is relevant for the introduction of the first assumption made

[1]To prevent confusion between the target nucleus and the compound system (the projectile-target combination), the $*$ notation is used in this paper for the compound system such that A (mass number)*.

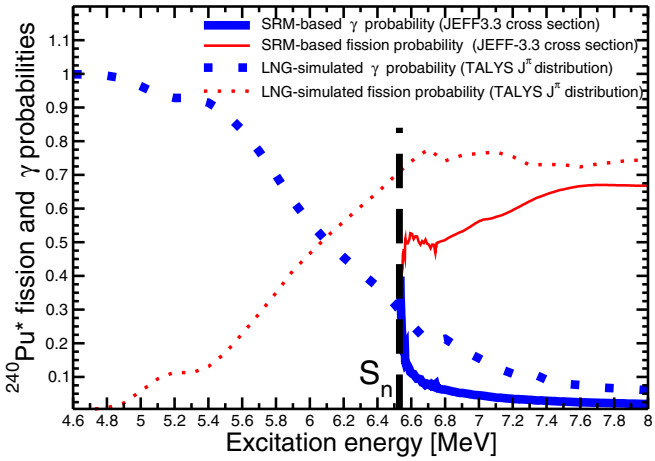

FIG. 1. Calculated fission and γ probabilities for the ^{240}Pu$(\alpha,\alpha')^{240}$Pu* reaction as a function of excitation energy of the compound system. The neutron-emission threshold (S_n), marked as a dashed vertical line, provides the neutron-scaled baseline. SRM-based estimates are represented by the solid curves, to be compared to present calculations performed with our AVXSF-LNG code (dotted lines).

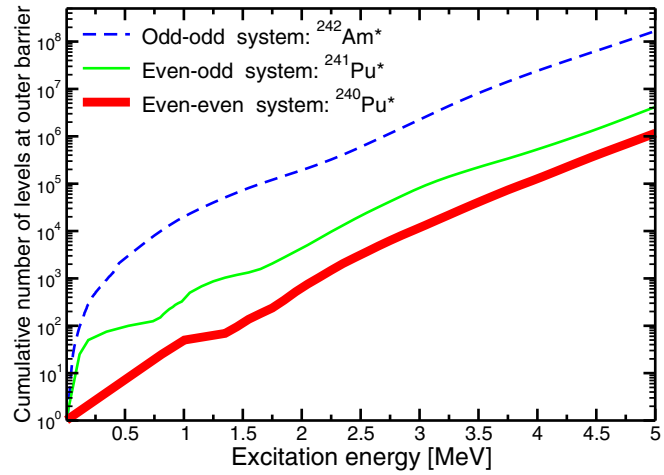

FIG. 2. Cumulative number of levels as a function of the excitation energy on top of the outer fission barrier for e-e (^{240}Pu*, red thick solid curve), odd-A (^{241}Pu*, green thin solid curve), and o-o (^{242}Am*, blue dashed curve) nuclei. These calculations are performed using the combinatorial quasiparticle-vibrational-rotational level density method developed in Ref. [25].

by the SRM, that states the J^π spin-parity independence of either the entrance-channel distribution (across $\mathcal{F}^{A^*}_{\rm surr}$) or the deexcitation-channel branching ratio ($\mathcal{B}^{J^\pi}_{c'}$ factor); the branching-ratio spin-parity independence hypothesis is also known as the Weisskopf-Ewing limit [29].

A. Fission channel

Following the historical introduction of the SRM, we first need to clarify the performances obtained in terms of neutron-induced fission cross section ($\sigma_{n,f}$) inference. Although the SRM had indisputable successes in matters of $\sigma_{n,f}$ reproduction and prediction, a recent reexamination [26] of fission probability data based on the R matrix approach demonstrated that this general observation must be tempered for even-even (e-e) fissioning compound systems and even more for the peculiar ^{240}Pu*. Figure 1 shows calculations of γ-ray emission and fission probabilities induced by the ^{240}Pu$(\alpha,\alpha')^{240}$Pu* direct reaction.[2] The profile of those probabilities is predicted by using two approaches: a *reference* one-dimensional fission barrier extended R-matrix calculation performed with the AVXSF-LNG code [25,26] and the straightforward SRM estimate. For the latter, the probability is retrieved in the spirit of Eq. (1), from the ratio of the deexcitation channel cross section $\sigma_{n,c'}$, reconstructed from the JEFF-3.3 neutron data evaluated library [31] divided by σ_n^{CN} as provided by an ECIS-06 optical-model coupled-channel calculation driven by the TALYS code [32]. In that sense, consistency is achieved with the reference calculation since the latter is here "fed" with the ^{240}Pu* spin-parity excited level distribution, $\mathcal{F}^{^{240}\mathrm{Pu}^*}_{\rm surr}(E_x,J^\pi)$, computed by the TALYS code [32]. The reference calculation accuracy is evaluated to $\pm 10\%$ [21], a value that is accurate enough to illustrate the failure of the SRM fission probability estimate for an e-e fissioning system. This failure is maximized in the special case of ^{240}Pu* (visible in the Fig. 1 by comparing the thin red curves with each other). Proper understanding of the latter statement requires us to comment on the results obtained by the AVXSF-LNG code, the full description of which is given in Refs. [25,26].

For fission, Eq. (2) becomes more complex and an appropriate formulation is given by Eq. (25) of Ref. [26]. For our present understanding, one takes the fission branching ratio as $\mathcal{B}^{J^\pi}_{c'} \simeq \sum_{\mu\in J^\pi}\mathcal{B}^{\mu}_{f}(E_x)$, with μ referring to any J^π fission transition channel (in the sense of A. Bohr [4]), lying on top of the outer hump of a one-dimensional potential barrier of the fissioning nucleus. On the basis of Eq. (2), we can discuss the disagreement observed in Fig. 1 in terms of fission probability between the SRM-based estimate and the reference calculation. Since low-energy fission occurs by barrier tunneling preferentially through the discrete sequence of transition states, the denser is the low-energy spectrum of the transition states, the less important the spin-parity dependence (stated by the SRM) of the fission branching ratio is. We can now anticipate the major reason for the failure of the SRM when applied to the e-e nuclei since their low-energy spectrum is built solely from pure collective intrinsic excitations [26], whereas odd-A and odd-odd (o-o) nuclei are characterized by low excitation energy combination of single-quasinucleon states with collective vibrations, involving necessarily a much denser sequence of transition states. This increase in complexity of the low-energy spectrum when moving from e-e to o-o nuclei is illustrated in Fig. 2 by combinatorial quasiparticle-vibrational-rotational level density calculations [25] for the ^{240}Pu*, ^{241}Pu*, and ^{242}Am* compound systems. The special spectrum pattern of e-e nuclei is even more enhanced for the peculiar ^{240}Pu* since its low-energy neutron fission shows

[2]The choice of this direct inelastic scattering reaction is made on purpose because of a recently performed measurement [30].

a very small opening according to the 1^+ s-wave fission channel[3] and is therefore essentially ruled by a few $J^\pi = 0^+$ transition channels. As a conclusion to this section, it is nowadays clear that fission of e-e nuclei occurring across a few vibrational excitations with rotational bands cannot fulfill the Weisskopf-Ewing limit hypothesis. Indeed, until recently, both calculations and data lacked the needed precision for a meaningful comparison (early study [34] is very representative of the two aspects).

B. γ-ray emission channel

Since the issue on fission is now settled, we can move on to the question of the inference of the neutron-capture cross section from direct-reaction γ-ray emission probability measurements. Figure 1 illustrates the systematic failure of the SRM applied to the observed γ-ray probability (thick solid curve). To deal with this question, we have selected the simpler case of a nonfissile nucleus: ^{176}Lu*. In addition the choice of this rare-earth nucleus is motivated by the following two arguments. First, the neutron-induced radiative-capture cross section of ^{175}Lu is well known, with average neutron resonance parameters recently evaluated [35], and second, precise γ-ray emission probability data [16] resulting from the ^{174}Yb(^{3}He, $p\gamma$)^{176}Lu* transfer reaction over the excitation range $[S_n - 0.76, S_n + 1.00]$ MeV are available. *Demonstrating the consistency between those probability data and the corresponding neutron cross section is the next challenge we address in this paper.*

For ^{176}Lu*, Eq. (2) is suitable to reproduce γ-ray emission probability data. Best prediction of those probabilities relies on the proper treatment of

(i) $\mathcal{F}^{^{176}Lu^*}_{\rm surr}(E_x, J^\pi)$, the spin-parity distribution of the compound system formed by the ^{174}Yb(^{3}He, p) reaction,
(ii) $\mathcal{B}^{J^\pi}_\gamma(E_x)$, the branching ratio regarding the ^{176}Lu* deexcitation via γ-ray emission, and
(iii) $W^{J^\pi}_{{\rm surr},\gamma}(E_x)$, the surrogate-dedicated channel width fluctuation correction factor for the (^{3}He, $p\gamma$) transfer reaction.

Demonstration has been made in [18,19] that considerable progress is ongoing in the extraction of information from the measured γ-ray emission probabilities by referring to a modified form of Eq. (1) in which the branching ratio is J^π dependent. It reads

$$\sigma^{HF}_{n,c'}(E_n) = \sum_{J^\pi} \sigma^{CN}_n(E_x, J^\pi)\mathcal{B}^{CN}_{c'}(E_x, J^\pi), \quad \text{with } c' \equiv \gamma. \tag{3}$$

Equation (3) is also known as the Hauser-Feshbach (HF) formula uncorrected for channel width fluctuations [36]. This equation is used to infer the neutron capture cross section jointly with $\mathcal{B}^{CN}_{c'}(E_x, J^\pi)$ *now computed* from the analysis of the measured γ-ray emission probability in the model of Eq. (2), in which the $W^{J^\pi}_{{\rm surr},c'\equiv\gamma}(E_x)$ factor has been neglected.

A large part of the progress in [18,19] has been made possible by the capability of confidently modeling the factor $\mathcal{F}^{A^*}_{\rm surr}(E_x, J^\pi)$ [Eq. (2)], relevant to the direct reaction selected for the nuclear surrogate-reaction measurement. However, a step further in terms of accuracy must be expected by the inclusion of the channel width fluctuation correction factors, *a step further that has been taken in this paper*.

The whole procedure relies on the coupling of two equations, the deexcitation probability and the cross section equations, that characterize the same excited compound system A^*. Those equations depend on a unique set of nuclear structure parameters. It reads, for the γ deexcitation channel,

$$\sigma_{n,\gamma}(E_n) = \sum_{J^\pi} \sigma^{A^*}_n(E_n, J^\pi)\mathcal{B}^{J^\pi}_\gamma(E_x)W^{J^\pi}_{n,\gamma}(E_n), \tag{4}$$

$$\mathcal{P}^{A^*}_{{\rm surr},\gamma}(E_x) = \sum_{J^\pi} \mathcal{F}^{A^*}_{\rm surr}(E_x, J^\pi)\mathcal{B}^{J^\pi}_\gamma(E_x)W^{J^\pi}_{{\rm surr},\gamma}(E_x). \tag{5}$$

The above equations provide the right framework for an accurate extraction of nuclear properties from measured neutron-induced cross section and/or direct-reaction induced probabilities in the fluctuating energy range. Among the various quantities involved are $W^{J^\pi}_{n,\gamma}(E_n)$ and $W^{J^\pi}_{{\rm surr},\gamma}(E_x)$, expressions that are well-known for the former [28] and recently outlined for the latter [26]. For ^{176}Lu*, the overall pattern (spin-parity integrated) is displayed in Fig. 3 as a function of the compound system excitation energy. We recognize the well-known profile of the customary incoming-outgoing channel width fluctuation correction factors [labelled WFCF in Fig. 3(a)] that shows the usual elastic enhancement with $W_{n,n_{\rm ground}}$ as large as 1.6 at 6.9 MeV. This elastic channel enhancement is strongly supported by the flux borrowed from the inelastic channels ($0.6 < W_{n,n'} < 1$) and, to a lesser extent, from the radiative channel. In contrast, the pattern of the surrogate-dedicated WFCF [labeled SWFCF in Fig. 3(b)], in which by concept no significant elastic scattering correlation is expected [26], highlights the new role of the radiative channel that endorses the enhancement pattern (up to +10%). From those distinct behaviors, one understands the importance of treating each width fluctuation correction factor in the calculation to reproduce without any bias the measured γ-ray emission probability.

We have calculated $\mathcal{P}^{^{176}Lu^*}_{{\rm surr},\gamma}$ from Eq. (5) using both the recently evaluated average parameters [35] of the (n + ^{176}Lu*) reaction and the spin-parity distribution of [16] (Fig. 8) that is characterized by an average spin of $\overline{J} = (7.1 \pm 0.05)\hbar$ with a standard deviation of $(2.3 \pm 0.1)\hbar$. Figure 4 shows the resulting γ-ray emission probability (dashed curve) in comparison with the two experimental data sets of [16]. One can already see a significant improvement in the calculation by comparison with the SRM-based prediction (thick solid curve). However, there is still an overestimation compared to the experimental data. Drawing conclusions requires one to recall that the spin-parity distribution we use here results from the best fit

[3]This statement is made according to the observed ^{240}Pu* ratio between the two s-wave average fission widths, meaning $\Gamma^{1+}_f/\Gamma^{0+}_f = 0.015$ (referring to Table I of [33]).

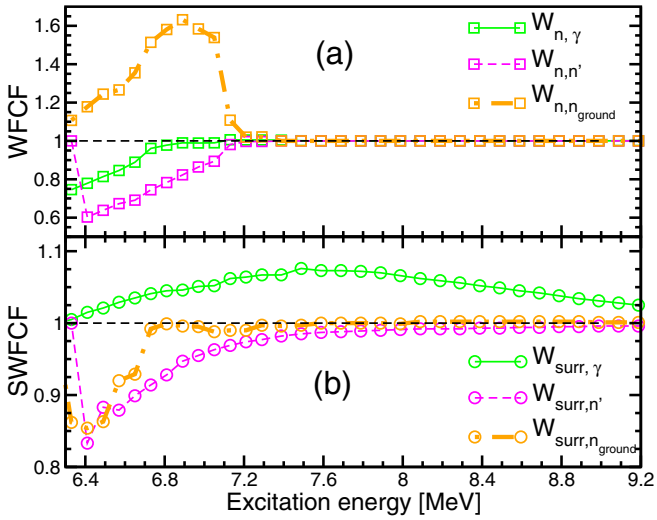

FIG. 3. Pattern comparisons of the width fluctuation correction factors as a function of the ^{176}Lu* excitation energy. (a) shows the $W_{n,\gamma}$, $W_{n,n'}$, and $W_{n,n_{\rm ground}}$ factors (called WFCF) involved in the calculation of the neutron-induced average cross sections of ^{175}Lu. (b) displays, by contrast, the specific pattern of the $W_{{\rm surr},\gamma}$, $W_{{\rm surr},n'}$, and $W_{{\rm surr},n_{\rm ground}}$ factors, called SWFCF, as triggered by the computation of probabilities [Eq. (5)]. Those factors, here, correspond to the spin-parity distribution of [16] (Fig. 8) that is characterized by an average spin of $\overline{J} = 7.1\hbar$ with a standard deviation of $\Delta\sigma = 2.3\hbar$. The high mean spin value and the wideness of the distribution are responsible for both the limited value of the maximum enhancement (+8%) and the very wide energy range spanned (about 3 MeV) until the customary high-energy pattern is recovered when the total number of deexcitation channels opened becomes very large, all the SWFCF tending thus to unity.

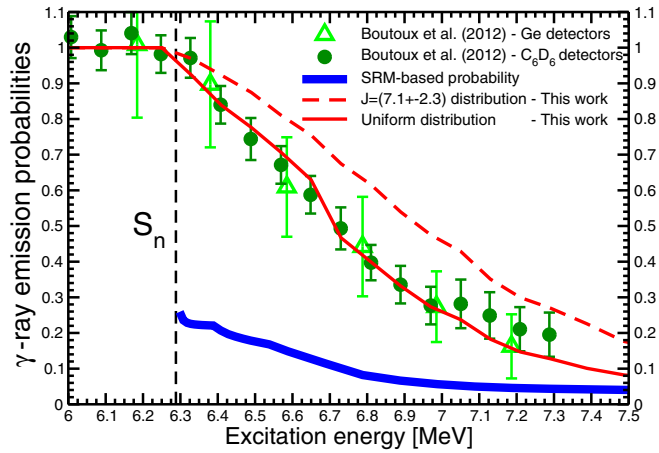

FIG. 4. Predicted and measured γ-ray emission probabilities for the ^{174}Yb(^{3}He, p) direct reaction as a function of compound system excitation energy. The neutron emission threshold (S_n), shown as a dashed vertical line, provides the neutron-scaled baseline. The measurement by Boutoux *et al.* [16] was performed using both C_6D_6 detectors (the dots) and germanium detectors (the triangles). The SRM-based calculation is represented by the solid thick line, to be compared with two simulations performed by the AVXSF-LNG CODE [25,26] using respectively a uniform spin-parity entrance distribution (thin solid line) and the distribution resulting from the fit of [16] (dashed line).

of $\mathcal{P}^{^{176}Lu^*}_{{\rm surr},\gamma}$ made by the authors of the experiment [16]. More precisely, they used the TALYS code [32] to reproduce the measured $\mathcal{P}^{^{176}Lu^*}_{{\rm surr},\gamma}$ data from the nuclear properties established, similarly to the present calculation, on the basis of the evaluated neutron capture cross section of ^{175}Lu (Fig. 4 of [16]). What differentiates in particular the present procedure from the original TALYS-based approach is the absence of a SWFCF term in the TALYS calculation. *By using the three-factor equation [Eq. (5)], the present work points out a possible bias in the fitted distribution in [16].* A fair agreement (Fig. 4, thin solid line) between the experimental data and the calculation is here obtained using a *uniform* spin-equiprobable-parity distribution that satisfies the relationship $\mathcal{F}^{^{176}Lu^*}_{\rm surr}(E_x, J^\pi) = \mathbb{1}/N_{J^\pi}\ \forall\, J^\pi$, with N_{J^π} the maximum number of J^π chosen in the distribution.

In the present study, we did not try to predict, using the most reliable theory, the J^π distribution relevant to the direct reaction that induces the γ-ray emission of ^{176}Lu*. This ability has been well demonstrated in [18] and [37] for the (p, d) and (n, n') direct reactions, respectively. We rather want to demonstrate now, using the coupled three-factor-equations [Eqs. (4) and (5)], our true capability to infer with reasonable accuracy any unknown quantity among $\sigma_{n,\gamma}$, $\mathcal{P}^{A^*}_{{\rm surr},\gamma}$, $\mathcal{B}^{J^\pi}_{\gamma}$, and $\mathcal{F}^{A^*}_{\rm surr}$ with the remaining variables $\sigma^{A^*}_{n}$, $W^{J^\pi}_{n,\gamma}$, and $W^{J^\pi}_{{\rm surr},\gamma}$ being nowadays assessed. Demonstration has been made above that the knowledge of all quantities except one, which in present case was the spin-parity distribution, can provide valuable feedback on the missing information.

III. FROM SRM TO EXTENDED SRM (ESRM)

The final section of this paper aims to anticipate the next move in the "art" of neutron cross section data evaluation. We realize that the future assimilation of direct-reaction induced probability data in the standard evaluation process is naturally conditioned on the resolution of the coupled equations (4) and (5) with an extended experimental database that will include the two types of observables; namely the surrogate nuclear reaction probabilities and the neutron-induced cross sections. We put much hope in this step further to address the neutron cross section target uncertainty as listed by Table I.

For the above "cumbersome" experimental data assimilation process, this paper aims to provide an alternative expression, accurate enough, to convert the measured direct-reaction induced probability into a *pseudo experimental* neutron cross section. The latter will be directly included in the standard database of observed cross sections to adjust the various parameters of the model. This data transformation, named after the SRM as *extended SRM*, is ruled by the

following equivalence:

$$\sigma_{n,c'}^{\text{ESRM}}(E_n) \simeq \sigma_{\mathbf{n}}^{\mathbf{A}^*}(\mathbf{E_n})\, \mathcal{P}_{\text{surr},\mathbf{c}'}^{\mathbf{A}^*}(\mathbf{E_x}) \left[\frac{\mathcal{P}_{\text{surr},c'}^{n\text{-dist.}}(E_x)}{\mathcal{P}_{\text{surr},c'}^{\text{fit-dist.}}(E_x)}\right] \left[\frac{W_{n,c'}^{n\text{-dist.}}(E_n)}{W_{\text{surr},c'}^{n\text{-dist.}}(E_x)}\right] \quad \text{with } c' \equiv \gamma, f, n, \text{ etc.} \tag{6}$$

Equation (6) is based on the Hauser-Feshbach formalism [27] following from the disjoined results of Eqs. (4) and (5), running for the latter two different distributions [the relevant neutron distribution (*n-fit*) and the best-suited distribution (*fit-dist*)]. Therefore, prior to the conversion, a fit of the spin-parity entrance distribution to the measured probability data is required using Eq. (5) to supply the best-suited distribution. The branching-ratio quantities are calculated using the best knowledge of the structural properties of the compound system. Computing Eq. (5) calls for two comments: (1) The determination of the most physical spin-parity distribution is not an essential condition; only the distribution to obtain the best agreement between the calculation and the model is. (2) The fit of the distribution requires a new calculation of the $W_{\text{surr},c'}^{J^\pi}$ factor at each iteration since the SWFCF pattern is indeed distribution dependent.

Finally, Eq. (6) looks pretty familiar since one recognizes, on the right, the standard SRM terms (in bold) of Eq. (1). The third term $[\mathcal{P}_{\text{surr},c'}^{n\text{-dist.}}/\mathcal{P}_{\text{surr},c'}^{fit\text{-dist.}}]$ and fourth term $[W_{n,c'}^{n\text{-dist.}}/W_{\text{surr},c'}^{n\text{-dist.}}]$, both new, are coefficients accounting for the differences in the neutron and direct-reaction spectroscopies. The efficiency of the ESRM transformation (with $c' \equiv \gamma$) is exemplified in Fig. 5. It shows the two experimental probability data sets [plots 5(b) and 5(c)] of [16] converted to pseudo experimental radiative neutron capture cross sections. The converted data are in good agreement with the associated AVXSF-LNG pointwise calculation, averaged over the energy-resolution bin attached to each experimental setup. As reference, the pointwise calculation is displayed against the directly measured neutron capture cross sections [38–40] [plot 5(a)]. We emphasize that no awkward normalization factor has been applied to achieve the observed agreement of the calculation and the experimental cross sections. We therefore fulfill the objective we set in the beginning of this study.

IV. SUMMARY AND PERSPECTIVES

In conclusion, demonstration is made in this paper that

(1) The direct-reaction induced γ-ray emission probability is compatible with the neutron spectroscopy radiative-capture cross section.
(2) The comparison between deexcitation probabilities and neutron induced cross sections has to be performed with the most accurate formalism; *including in particular the SWFCF term for the deexcitation probability*. The ESRM expression in that sense outdates the historical SRM,
(3) The γ-ray emission probability provides valuable information in the energy range where neutron-spectroscopy radiative-capture cross section measurements still represent an experimental challenge ($E_n > 200$ keV),
(4) The measured direct-reaction γ-ray emission probability provides stringent constraints on the evaluation of either the neutron capture cross section or the nuclear structure properties depending on the unknown quantity when solving Eqs. (4) and (5).

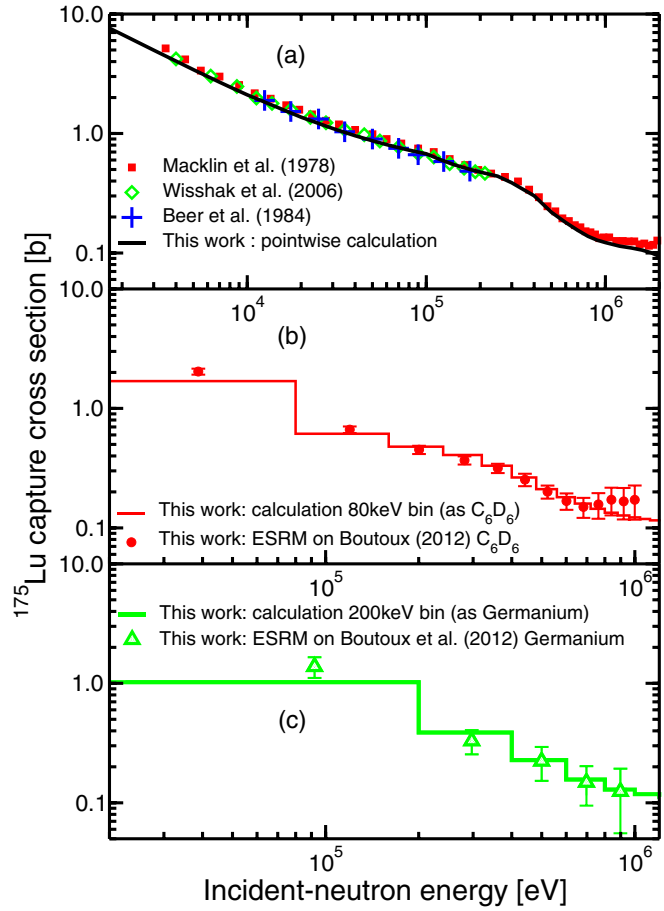

FIG. 5. Radiative-capture cross section of the ^{175}Lu target nucleus as a function of the incident-neutron energy. (a) displays the comparison between the cross section calculated in this work (solid curve, consistent with the evaluation of [35] that used the TALYS code) and the neutron spectroscopy measurements by Wisshak *et al.* [38], Macklin *et al.* [39], and Beer *et al.* [40]. (b) and (c) show the comparisons of the same calculation but, respectively, averaged over the 80 and 200 keV constant bin widths as done by Boutoux *et al.* [16] in their experiment. The latter was performed using two independent experimental methods based on the use of C_6D_6 scintillators and germanium detectors. The high bin width value (200 keV) quoted for the germanium data was chosen to lower statistical errors. The comparison in (a) and (b) of the present calculation is made with the ESRM transformation of the γ-ray emission probability data set from Boutoux *et al.* [16].

The present study, somehow, terminates a twenty-year-old-standing debate on the kind of feedback one should expect from surrogate-reaction probability measurements. Demonstration is being made that, in the near future, accurate-enough information will be extracted from probability data to deal with the increasing needs in neutron reactor physics data and to provide the requisite nuclear physics input for studies of the structure of unstable nuclei involved in astrophysics. The proposed ESRM comes in time for a full assimilation of next-generation direct-reaction probability data to be measured in brand new experimental facilities [41,42]. These promising facilities, based on inverse kinematics with radioactive ion beams, will allow simultaneous accurate measurements of direct-reaction induced-fission, γ-ray, and neutron-emission probabilities. By jointly analyzing probability and cross section data, the ESRM is able to unify the cross section evaluation techniques in use in nuclear physics.

ACKNOWLEDGMENTS

One of the authors (O.B.) expresses his deep gratitude to E. J. Lynn from LANL/T-2 for numerous fruitful discussions on physics related to surrogate nuclear reactions. The authors would like to warmly thank P. Marini from CENBG/CNRS and M. Diakaki from CEA/IRESNE for a very careful reading of the manuscript. Special thanks go to G. Boutoux from CEA/CESTA for complementary experimental information. We are profoundly grateful to L. C. Leal from IRSN (France) for providing the final touch to this document.

[1] E. O. Lawrence, E. McMillan, and R. L. Thornton, Phys. Rev. **48**, 493 (1935).
[2] J. D. Cramer and H. C. Britt, Nucl. Sci. Eng. **41**, 177 (1970).
[3] V. M. Strutinsky, Nucl. Phys. A **95**, 420 (1967).
[4] A. Bohr and B. R. Mottelson, Phys. Rev. **90**, 717 (1953).
[5] H. C. Britt and J. B. Wilhelmy, Nucl. Sci. Eng. **72**, 222 (1979).
[6] W. Younes and H. C. Britt, Phys. Rev. C **67**, 024610 (2003).
[7] W. Younes and H. C. Britt, Phys. Rev. C **68**, 034610 (2003).
[8] M. Petit, M. Aiche, G. Barreau, S. Boyer, N. Carjan, S. Czajkowski, D. Dassié, C. Grosjean, A. Guiral, B. Haas *et al.*, Nucl. Phys. A **735**, 345 (2004).
[9] G. Kessedjian, B. Jurado, G. Barreau, P. Marini, L. Mathieu, I. Tsekhanovich, M. Aïche, G. Boutoux, S. Czajkowski, and Q. Ducasse, Phys. Rev. C **91**, 044607 (2015).
[10] P. Archier, C. De Saint Jean, G. Noguere, O. Litaize, P. Leconte, and C. Bouret, in *Proceedings of the International Conference on the Physics of Reactors (PHYSOR 2014), Sep. 28–Oct. 3, 2014, Kyoto, Japan*, edited by K. Suyam, T. Sugawara, K. Tada, G. Chiba, and A. Yamamoto, Report No. JAEA-Conf 2014-003.
[11] A. J. Koning, J. Blomgren, R. Jacqmin, A. J. M. Plompen, R. Mills, G. Rimpault, E. Bauge, D. Cano Ott, S. Czifrus, K. Dahlbacka, I. Goncalves, H. Henriksson, D. Lecarpentier, E. Malambu Mbala, V. Stary, C. Trakas, and C. Zimmerman, Nuclear data for sustainable nuclear energy, JRC Report No. EUR 23977, 2009 (unpublished).
[12] B. S. Meyer, Annu. Rev. Astron. Astrophys. **32**, 153 (1994).
[13] O. Cabellos, P. Fernandez, D. Rapisarda, and N. Garcia-Herranz, Nucl. Instrum. Methods Phys. Res., Sect. A **618**, 248 (2010).
[14] J. L. Ullmann, T. Kawano, T. A. Bredeweg, A. Couture, R. C. Haight, M. Jandel, J. M. O'Donnell, R. S. Rundberg, D. J. Vieira, J. B. Wilhelmy *et al.*, Phys. Rev. C **89**, 034603 (2014).
[15] M. Guttormsen, L. A. Bernstein, A. Bürger, A. Görgen, F. Gunsing, T. W. Hagen, A. C. Larsen, T. Renstrøm, S. Siem, M. Wiedeking, and J. N. Wilson, Phys. Rev. Lett. **109**, 162503 (2012).
[16] G. Boutoux, B. Jurado, V. Méot, O. Roig, L. Mathieu, M. Aïche, G. Barreau, N. Capellan, I. Companis, S. Czajkowski *et al.*, Phys. Lett. B **712**, 319 (2012).
[17] Q. Ducasse, B. Jurado, M. Aiche, P. Marini, L. Mathieu, A. Görgen, M. Guttormsen, A. C. Larsen, T. Tornyi, J. N. Wilson *et al.*, Phys. Rev. C **94**, 024614 (2016).
[18] J. E. Escher, J. T. Burke, R. O. Hughes, N. D. Scielzo, R. J. Casperson, S. Ota, H. I. Park, A. Saastamoinen, and T. J. Ross, Phys. Rev. Lett. **121**, 052501 (2018).
[19] A. Ratkiewicz, J. A. Cizewski, J. E. Escher, G. Potel, J. T. Burke, R. J. Casperson, M. McCleskey, R. A. E. Austin, S. Burcher, R. O. Hughes *et al.*, Phys. Rev. Lett. **122**, 052502 (2019).
[20] R. Pérez Sánchez, B. Jurado, P. Marini, M. Aiche, S. Czajkowski, D. Denis-Petit, Q. Ducasse, L. Mathieu, I. Tsekhanovich, A. Henriques, V. Méot, and O. Roig, Nucl. Instrum. Methods Phys. Res., Sect. A **933**, 63 (2019).
[21] O. Bouland (unpublished).
[22] J. E. Escher, J. T. Burke, F. S. Dietrich, N. D. Scielzo, I. J. Thompson, and W. Younes, Rev. Mod. Phys. **84**, 353 (2012).
[23] A. J. Koning and J. P. Delaroche, Nucl. Phys. A **713**, 231 (2003).
[24] E. Sh. Soukhovitskii, S. Chiba, J.-Y. Lee, O. Iwamoto, and T. Fukahori, J. Phys. G: Nucl. Part. Phys. **30**, 905 (2004).
[25] O. Bouland, J. E. Lynn, and P. Talou, Phys. Rev. C **88**, 054612 (2013).
[26] O. Bouland, Phys. Rev. C **100**, 064611 (2019).
[27] W. Hauser and H. Feshbach, Phys. Rev. **87**, 366 (1952).
[28] S. Hilaire, Ch. Lagrange, and A. J. Koning, Ann. Phys. (NY) **306**, 209 (2003).
[29] V. F. Weisskopf and D. H. Ewing, Phys. Rev. **57**, 472 (1940).
[30] R. Pérez Sánchez, B. Jurado, V. Méot, O. Roig, M. Dupuis, O. Bouland, D. Denis-Petit, P. Marini, L. Mathieu, I. Tsekhanovich *et al.*, Phys. Rev. Lett. **125**, 122502 (2020)
[31] O. Cabellos, F. Alvarez-Velarde, M. Angelone, C. J. Diez, J. Dyrda, L. Fiorito, U. Fischer, M. Fleming, W. Haeck, I. Hill *et al.*, EPJ Web Conf. **146**, 06004 (2017).
[32] A. J. Koning, S. Hilaire, and M. C. Duijvestijn, in *Proceedings of the International Conference on Nuclear Data for Science and Technology - ND2007, May 22–27, 2007, Nice, France*, edited by O. Bersillon *et al.* (EDP Sciences, Les Ulis, France, 2008), pp. 211–214.
[33] J. E. Lynn, P. Talou, and O. Bouland, Phys. Rev. C **97**, 064601 (2018).
[34] B. B. Back, O. Hansen, H. C. Britt, and J. D. Garrett, Phys. Rev. C **9**, 1924 (1974).
[35] G. Noguere, O. Bouland, J. Heyse, S. Kopecky, C. Paradela, P. Schillebeeckx, A. Ebran, and O. Roig, Phys. Rev. C **100**, 065806 (2019).

[36] P. A. Moldauer, Phys. Rev. C **11**, 426 (1975).
[37] M. Dupuis, E. Bauge, S. Hilaire, F. Lechaftois, S. Péru, N. Pillet, and C. Robin, Eur. Phys. J. A **51**, 168 (2015).
[38] K. Wisshak, F. Voss, F. Käppeler, M. Krtička, S. Raman, A. Mengoni, and R. Gallino, Phys. Rev. C **73**, 015802 (2006).
[39] R. L. Macklin, D. M. Drake, and J. J. Malanify, Los Alamos National Laboratory Report No. LASL, 1978. 2P. (LA-7479-MS).
[40] H. Beer, G. Walter, R. L. Macklin, and P. J. Patchett, Phys. Rev. C **30**, 464 (1984).
[41] R. Reifarth, S. Altstadt, K. Göbel, T. Heftrich, M. Heil, A. Koloczek, C. Langer, R. Plag, M. Pohl, K. Sonnabend *et al.*, J. Phys.: Conf. Ser. **665**, 012044 (2016).
[42] R. Reifarth, K. Göbel, T. Heftrich, M. Weigand, B. Jurado, F. Käppeler, and Y. Litvinov, Phys. Rev. Accel. Beams **20**, 044701 (2017).